Scientia Iranica (2024) 31(13), 967–979

Sharif University of Technology
Scientia Iranica
Transactions B: Mechanical Engineering
https://scientiairanica.sharif.edu

Minimum stiffness and optimal position of intermediate elastic support to maximize the fundamental frequency of a vibrating Timoshenko beam

H. Ebrahimi, F. Kakavand*, and H. Seidi

Department of Mechanical Engineering, Takestan Branch, Islamic Azad University, Takestan, Iran.

Received 8 November 2021; received in revised form 16 November 2022; accepted 21 May 2023

KEYWORDS
Euler-Bernoulli; Intermediate support; Optimal position; Minimum stiffness; Finite element method.

Abstract. The optimal position and minimum support stiffness of a vibrating Timoshenko beam are investigated to maximize the fundamental frequency. The finite element method is employed. According to the maximum-minimum theorem of Courant, the optimum position is at the zero of the second mode shape function. The intermediate support's position and minimal stiffness for a wide variety of slenderness proportions were achieved. It was observed that the ideal position of intermediate support and its minimum stiffness are sensitive to the slenderness ratio. Also, for thick cantilever beams with intermediate support at the optimal location, the minimum support stiffness is less than 266.9, which was reported in the literature for the Euler-Bernoulli beam. The minimum stiffness of familiar end conditions of an optimally located beam is presented for a wide range of slenderness ratios. Since, in many practical applications, it is impossible to locate support at the optimal position, the minimum support stiffness for a beam in which its intermediate support is not located at the optimal position is obtained for various boundary conditions and slenderness ratios. Furthermore, empirical evaluations were carried out, and the findings were contrasted with hypothetical estimates of the initial two natural frequencies.

1. Introduction

A beam is applied in several engineering structures, such as industrial mixers and robotic manipulators, particularly in bridges, buildings, and supporting structures. Understanding the modal characteristics of the beam is essential for avoiding resonance. By adding intermediate support, we can improve its modal characteristics.

In addition to being required to maintain a structure solidly, supports can be extremely important to the stability and understanding of structural dynamics. A slight change to the stiffness or position of intermediate support can dramatically influence the natural

*. *Corresponding author.*
E-mail addresses: Hossein_ebrahimi11@yahoo.com (H. Ebrahimi); F.kakavand@gmail.com (F. Kakavand); Hseidi@yahoo.com (H. Seidi)

To cite this article:
H. Ebrahimi, F. Kakavand, and H. Seidi "Minimum stiffness and optimal position of intermediate elastic support to maximize the fundamental frequency of a vibrating Timoshenko beam", *Scientia Iranica* (2024), **31**(13), pp. 967-979
https://doi.org/10.24200/sci.2023.59366.6196

frequencies and critical buckling load, significantly improving the structural performance.

Courant [1] stated that the addition of n kinematic limitations to a system will result in new eigenvalues which satisfy the following inequalities:

$$\lambda_{i+n} \leq \sigma_i \leq \lambda_{i+n+1},$$

σ_i is the ith eigenvalue of the constrained system, and λ_i is the ith eigenvalue of the unconstrained system [2]. The maximum-minimum theorem of Courant indicated how n kinematical constrained should be applied in order for the upper limit of the above inequality to be reached.

When the optimal position of an intermediate support is determined, according to Courant and Hilbert [3], the optimal point of the intermediate support is at the zero of the unrestricted beam's second mode shape function (ZSMS). Concerning a cantilever beam, it is 0.7834L. Based on the maximum-minimum theorem of Courant using intermediate support located at the optimal position, the constrained beam's first natural frequency equals the unconstrained cantilever beam's second natural frequency.

Because constructing support containing infinite stiffness is unachievable, the lowest stiffness of support necessary for maximizing natural frequency is of tremendous importance in engineering applications. Akesson and Olhoff [4] have shown that for an Euler-Bernoulli cantilever beam that was imposed by an optimally located elastic support, i.e., at 0.7834L, the increasing of support stiffness yields the increase of the fundamental frequency, but after passing a critical value which they called minimum stiffness, increasing of support stiffness does not affect fundamental frequency. They obtained this non-dimensionalized minimum stiffness with numerical methods as 266.9. Wang [5] obtained a minimum value of 266.87 by the analytical method and assumed a zero slope of mode shape at the optimal position.

The effect of intermediate supports on critical buckling loads and dynamic response are studied in many published papers response of beams. Olhoff and Åkesson [6] investigated the influence of different elastic support positions and stiffness on the frequency of the column buckling loads' greatest value. Rao [7] provided accurate and precise frequency and mode shape equations of the clamped both ends uniform beams with intermediate elastic support. The ideal support locations for a cantilever beam and a rectangular cantilever plate were determined using sensitivity analysis of eigenvalues by Won and Park [8]. With the endpoints elastically restricted against rotation and translation, Albaracin et al. [9] investigation focused on the uniform beam problem with intermediate restrictions. The support designs for layouts that relates to the optimization of boundary conditions were proposed by Zhu and Zhang [10] after their study to increase the structures' natural frequency. In order to reduce the maximum bending moment and increase the natural frequency, Wang et al. examined the best designs of structural support placements [11,12]. Support position optimization involving minimal stiffness regarding plate systems, such as support mass, was investigated by Wang and Friswell [13] in addition to the least support stiffness necessary to increase the plate systems' basic natural frequency. The basic frequency of plate was maximized by Kong [14] by analyzing the vibration of plates under different boundary and intermediate support positions. He then determined the best position and stiffness of discrete elastic supports. Wang et al. [15] discovered how to adjust the basic natural frequency of rectangular plates by locating the lowest possible stiffness of point support. Aydin studied cantilever beams backed up by optimum elastic springs to reduce dynamic deviations and surges [16] and the most effective distribution of elastic springs wherever a cantilever beam is mounted and minimizing the impact of shear force on the beam supporting [17]. For Euler-Bernoulli beams containing elastic support, Roncevic et al. [18] investigated the frequency equation and mode forms. Abdullatif and Mukherjee [19] analyzed the effect of intermediate support on the critical stability of a cantilever with non-conservative loading.

Due to the importance of the dynamic response of the beams with intermediate supports, some studies have been done on forced and natural vibrations on multi-span beams. Researchers studied the multi-span beams' axial vibrations having concentrated masses [20], multi-span beams' unconstrained vibration having flexible constraints [21], and the free and forced vibration characteristics of a Bernoulli-Euler multi-span beam carrying several different concentrated elements [22].

Among the studies performed to optimize the fundamental frequency and obtain the minimum stiffness of the intermediate support, providing an accurate solution method for determining the natural frequency and modes shape of the beam with intermediate supports for different boundary conditions has been the subject of interest to researchers. These methods have been performed for Euler-Bernoulli and Timoshenko beams. Laplace transform method [23], dynamic stiffness matrix method [24], and series expansion approach [25], the Green's Function Method (GFM) [26] implemented to confront the beams' vibration assessment having elastic supports or attachments include these methods. To determine the Euler-Bernoulli beams' natural frequencies and mode shapes, recent research by Roncevic et al. [27] compared the effectiveness of two analytical techniques (Laplace transform and GFM). They expanded the investigation by thor-

oughly addressing fifty-nine different boundary-setting combinations for beams backed up by translational springs [18]. Given an unpredictable frequency of intermediate elastic constraint, Luo et al. [28] propose a precise closed-form solution for unconstrained vibration of discretely supported Euler-Bernoulli and Timoshenko beams. The generalized function approach is employed to determine the accurate eigenvalue equations and mode shapes, extending the universal solution of mode forms as a blend of typical trigonometric/hyperbolic functions with incorporation constants expanded to generalized functions.

Most of the research on optimizing fundamental frequencies by adding intermediate support is founded on the Euler-Bernoulli beam theory. In addition, in many industrial applications, it is impossible to add support in the optimal location; hence the designer has to add support at other points. It is clear that the maximum limit of the first frequency, in this case, is the frequency corresponding to applying for the rigid support at that point.

This paper aims to study the effect of placing elastic supports at any location in thick and thin beams on the required stiffness and first natural frequency to optimize the fundamental frequencies of a C-F Timoshenko beam. The Finite Element Method (FEM) is applied to free vibration. The validity and accuracy of the results are evaluated through comparison to an analytical method and previous works. The optimization of the fundamental frequency was carried out by exploring the impact of the intermediate elastic support's position and stiffness on the fundamental frequency. This is clear that if we add support at a non-optimal position, the minimum stiffness will not exist. Therefore we considered a 5% tolerance zone to determine the minimum stiffness. The design curve is presented through the minimum stiffness and optimum frequency at different mass ratios.

This paper is organized as follows. In Sections 2, 3, and 4, we have established analytical models of the Euler-Bernoulli, Timoshenko, and FEM, respectively. In Section 5 the optimum position and the minimum stiffness of internal support based on the Timoshenko model was found and a comprehensive discussion about changing mode shape and variation of the second mode is presented. In addition, we suggest a tolerance zone to introduce a minimum stiffness for a beam with a non-optimally located internal support. In Section 6 experimental evaluation was done and the results were compared with analytical calculations. Finally in Section 7 ends the paper with some conclusions.

2. Euler-Bernoulli analytical model

A cantilever beam with intermediate elastic support

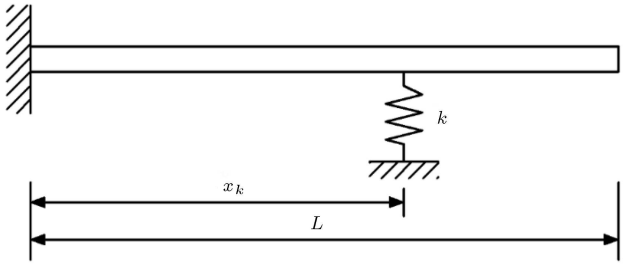

Figure 1. Cantilever beam with elastic intermediate support [5].

is located at a distance x_k from the clamp end, as shown in Figure 1. Based on Euler-Bernoulli theory, the governing equation for the vibration of the beam is as follows [29]:

$$EI\frac{\partial^4 w(x,t)}{\partial x^4} + \rho A\frac{\partial^2 w(x,t)}{\partial t^2} = 0, \tag{1}$$

where E, I, A, ρ, and $w(x,t)$ represent the elastic modulus, inertia moment, cross-section domain, density, and the deflection of the beam at cross-section x at time t, respectively. Considering simple harmonic motion, the solution of Eq. (1) is assumed as follows:

$$w(x,t) = W(x)e^{i\omega t}, \tag{2}$$

where $W(x)$ represents the mode shape function, and ω is the natural beam frequency. After replacing Eq. (2) with Eq. (1), the corresponding eigenvalue problem can be formulated as follows:

$$W^{(4)}(x) - \beta^4 W(x) = 0, \tag{3}$$

where $\beta^4 = \omega^2\rho A/EI$ is the dimensionless frequency parameter; the sub-functions in Eq. (3), the general solution of mode shapes can be written as:

$$W_1(x) = C_1\sin(\beta x) + C_2\cos(\beta x) + C_3\sinh(\beta x) + C_4\cosh(\beta x), \qquad 0 \le x \le x_k, \tag{4}$$

$$W_2(x) = C_5\sin(\beta x) + C_6\cos(\beta x) + C_7\sinh(\beta x) + C_8\cosh(\beta x), \qquad x_k \le x \le L. \tag{5}$$

The non-dimensionalized natural frequencies as β are defined throughout the paper either in the Timoshenko model or the Euler-Bernoulli model. To obtain constant coefficients C_1 to C_8 and natural frequencies, we have four boundary settings at both ends of the beam and four continuity and jump conditions at the junction point x_k. At the clamped end, the deflection and the slope are zero. The shear force and the bending moment are zero at the free end. As a result, the end boundary conditions of the beam will be as follows:

$$W_1(0) = W_1'(0) = W_2''(L) = W_2'''(L) = 0. \tag{6}$$

At point x_k, where the elastic support is located, the deflection, slope, and bending moment are continuous, and the shear force has a jump. Four boundary conditions at the junction point are:

$$W_1(x_k) = W_2(x_k), \qquad W_1{}'(x_k) = W_2{}'(x_k),$$

$$W_1{}''(x_k) = W_2{}''(x_k),$$

$$W_1{}'''(x_k) - W_2{}'''(x_k) = \frac{k}{EI} W_1(x_k). \tag{7}$$

Appling eight boundary conditions (6) and (7) to Eqs. (4) and (5) and establishing the corresponding characteristics equation, the natural frequencies and mode shapes will be found. For known values of and b, natural frequencies can be obtained from the characteristic equation.

3. Timoshenko model

The following are Timoshenko beam's unrestricted vibration equations [29]:

$$\rho A \frac{\partial^2 w(x,t)}{\partial t^2} - \mu AG \left(\frac{\partial^2 w(x,t)}{\partial x^2} - \frac{\partial \psi}{\partial x} \right) = 0, \tag{8a}$$

$$\rho I \frac{\partial^2 \psi(x,t)}{\partial t^2} - EI \frac{\partial^2 \psi(x,t)}{\partial x^2} - \mu AG \left(\frac{\partial w(x,t)}{\partial x} - \psi(x,t) \right) = 0, \tag{8b}$$

where μ the shear correction factor, w and ψ is indicate the beam axis's deflection and bending slope, respectively. Appling separation of the variable method, the mode shapes lead to:

$$\begin{bmatrix} W(x) \\ \Psi(x) \end{bmatrix} = \begin{bmatrix} C_1 \\ D_1 \end{bmatrix} \sin(ax) + \begin{bmatrix} C_2 \\ D_2 \end{bmatrix} \cos(ax) + \begin{bmatrix} C_3 \\ D_3 \end{bmatrix} \sinh(bx) + \begin{bmatrix} C_4 \\ D_4 \end{bmatrix} \cosh(bx), \tag{9}$$

where $W(x)$ and $\Psi(x)$ indicate the modal functions explaining the deflection and flexion slope, respectively. The coefficients α and b are related to ω, given by [29]:

$$a = \left[\frac{\rho\omega^2}{2\mu G} + \sqrt{\left(\frac{\rho\omega^2}{2\mu G} \right)^2 + \rho\omega^2} \right]^{1/2},$$

$$b = \left[-\frac{\rho\omega^2}{2\mu G} + \sqrt{\left(\frac{\rho\omega^2}{2\mu G} \right)^2 + \rho\omega^2} \right]^{1/2}. \tag{10}$$

The sub-functions of the spatial solution can be written as:

$$\begin{bmatrix} W_1(x) \\ \Psi_1(x) \end{bmatrix} = \begin{bmatrix} C_1 \\ D_1 \end{bmatrix} \sin(ax) + \begin{bmatrix} C_2 \\ D_2 \end{bmatrix} \cos(ax) + \begin{bmatrix} C_3 \\ D_3 \end{bmatrix} \sinh(bx) + \begin{bmatrix} C_4 \\ D_4 \end{bmatrix} \cosh(bx), \quad 0 \le x \le x_k,$$

$$\begin{bmatrix} W_2(x) \\ \Psi_2(x) \end{bmatrix} = \begin{bmatrix} C_5 \\ D_5 \end{bmatrix} \sin(ax) + \begin{bmatrix} C_6 \\ D_6 \end{bmatrix} \cos(ax) + \begin{bmatrix} C_7 \\ D_7 \end{bmatrix} \sinh(bx) + \begin{bmatrix} C_8 \\ D_8 \end{bmatrix} \cosh(bx), \quad x_k \le x \le L. \tag{11}$$

The coefficients C_i and D_i are related to each other. Similar to the previous section, eight boundary conditions can be written as follows:

$$W_1(0) = \Psi_1(0) = \Psi_2{}'(L) = \mu AG \left(W_2{}'(L) - \Psi_2(L) \right) = 0,$$

$$W_1(x_k) = W_2(x_k),$$

$$\Psi_1(x_k) = \Psi_2(x_k),$$

$$\Psi_1{}'(x_k) = \Psi_2{}'(x_k),$$

$$\mu AG \left(W_1{}'(x_k) - \Psi_1(x_k) \right) - \mu AG \left(W_2{}'(x_k) - \Psi_2(x_k) \right) = kW_1(x_k). \tag{12}$$

Consequently, the characteristic equation can be derived by imposing boundary conditions (12) to mode shape functions (11). The natural frequency and mode shape are obtained by solving the characteristic equation.

4. Finite Element Model (FEM)

In this section, the FEM is used to evaluate natural frequencies. For the Euler-Bernoulli beam, the deformation vector and shape functions are as follows [2,30]:

$$q_e = \{ w_e, \theta_e, w_{e+1}, \theta_{e+1} \}^T, \tag{13}$$

$$N_w = \frac{1}{h_e^3} \begin{bmatrix} (x - x_{e+1})^2 (2x - 3x_e + x_{e+1}) \\ h_e (x - x_e)(x - x_{e+1})^2 \\ -(x - x_e)^2 (2x + x_e - 3x_{e+1}) \\ h_e (x - x_e)^2 (x - x_{e+1}) \end{bmatrix}, \tag{14}$$

$$h_e = x_{e+1} - x_e, \tag{15}$$

$$N_w = \begin{bmatrix} -\frac{(x-x_{e+1})}{(x_e-x_{e+1})}\frac{(2\alpha x^2-\alpha x x_{e+1}-\alpha x_{e+1}^2+12)-3\alpha x_e(x-x_{e+1})}{(\alpha x_e^2-2\alpha x_e x_{e+1}+\alpha x_{e+1}^2-12)} \\ -\frac{(x-x_e)(x-x_{e+1})(\alpha x x_{e+1}-\alpha x x_e-\alpha x_{e+1}^2+\alpha x_e x_{e+1}+6)}{(x_e-x_{e+1})(\alpha x_e^2-2\alpha x_e x_{e+1}+\alpha x_{e+1}^2-12)} \\ \frac{(x-x_e)}{(x_e-x_{e+1})}\frac{(2\alpha x^2-\alpha x x_e-\alpha x_e^2+12)-3\alpha x_{e+1}(x-x_e)}{(\alpha x_e^2-2\alpha x_e x_{e+1}+\alpha x_{e+1}^2-12)} \\ \frac{(x-x_e)(x-x_{e+1})(\alpha x x_e-\alpha x_e^2-\alpha x x_{e+1}+\alpha x_e x_{e+1}+6)}{(x_e-x_{e+1})(\alpha x_e^2-2\alpha x_e x_{e+1}+\alpha x_{e+1}^2-12)} \end{bmatrix}, \tag{17}$$

$$N_\psi = \begin{bmatrix} -\frac{6\alpha(x-x_e)(x-x_{e+1})}{(x_e-x_{e+1})(\alpha x_e^2-2\alpha x_e x_{e+1}+\alpha x_{e+1}^2-12)} \\ \frac{(x-x_{e+1})}{(x_e-x_{e+1})}+\frac{3\alpha(x-x_e)(x-x_{e+1})}{(\alpha x_e^2-2\alpha x_e x_{e+1}+\alpha x_{e+1}^2-12)} \\ \frac{6\alpha(x-x_e)(x-x_{e+1})}{(x_e-x_{e+1})(\alpha x_e^2-2\alpha x_e x_{e+1}+\alpha x_{e+1}^2-12)} \\ -\frac{(x-x_e)}{(x_e-x_{e+1})}+\frac{3\alpha(x-x_e)(x-x_{e+1})}{(\alpha x_e^2-2\alpha x_e x_{e+1}+\alpha x_{e+1}^2-12)} \end{bmatrix}. \tag{18}$$

Box I

w_e, θ_e, w_{e+1}, and θ_{e+1} are deflection and slope at node "e" and "$e+1$" respectively. For Timoshenko Beam, deformation vector and shape functions are [30]:

$$q_e = \{w_e, \psi_e, w_{e+1}, \psi_{e+1}\}^T, \tag{16}$$

N_w and N_ψ are calculated as shown in Box I, where α is $\mu AG/EI$. Expressing a weak form of governing equations and imposing boundary conditions, one gets the equation for a single finite element in the following form:

$$m_e\ddot{q}_e + k_e q_e = 0. \tag{19}$$

Elemental matrixes for the Euler-Bernoulli model are:

$$k_e = \int_{x_e}^{x_{e+1}} EI\frac{d^2N_w}{dx^2}\frac{d^2N_w^T}{dx^2}dx, \tag{20}$$

$$m_e = \int_{x_e}^{x_{e+1}} \rho A N_w N_w^T dx. \tag{21}$$

Elemental matrixes for the Timoshenko model are:

$$k_e = \int_{x_e}^{x_{e+1}} \left(\mu AG\left(\frac{dN_w}{dx}-N_\psi\right)\left(\frac{dN_w}{dx}-N_\psi\right)^T + EI\frac{dN_\psi}{dx}\frac{dN_\psi^T}{dx}\right)dx, \tag{22}$$

$$m_e = \int_{x_e}^{x_{e+1}} \left(\rho A N_w N_w^T + \rho I N_\psi N_\psi^T\right)dx. \tag{23}$$

Obviously, the presence of elastic support will change the stiffness matrix of the corresponding element to which the spring is connected. Since the elastic support is not necessarily located at nodes, the additional elemental matrix corresponding to the element to which the elastic support is attached to will be as follows:

$$k_e^{Spring} = k\left[N_w N_w^T\right]\Big|_{x=x_k}. \tag{24}$$

This matrix should be added to the elemental matrix of the corresponding element. After the assembling process, one gets the following expression:

$$M\ddot{Q} + KQ = 0, \tag{25}$$

where, Q is the global deformation matrix for Euler Bernoulli and Timoshenko model. M and K are global mass and stiffness matrices, respectively. The solution of Eq. (25) is assumed to be harmonic as:

$$Q = \vec{X}e^{i\omega t}, \tag{26}$$

where $\vec{X}$ is the vector of amplitudes, and ω is the natural vibration frequency. Finally, the corresponding eigenvalue problem is:

$$\left([K] - \omega_i^2[M]\right)\vec{X}_i = \vec{0}. \tag{27}$$

The natural frequencies are the solution of the following characteristic equation:

$$\det\left([K] - \omega^2[M]\right) = 0. \tag{28}$$

5. Numerical results and discussion

For simplicity of numerical investigations and convenience of discussions, dimensionless parameters are introduced as follows:

$$K_s = \frac{kL^3}{EI}, \qquad \xi = \frac{x_k}{L}.$$

Figure 2 depicts the first mode shape of a cantilever beam having an intermediate elastic supporting with $K_s = 300$ at $\xi = 0.7834$. Mode shape was plotted for two L/R ratios, where R is the radius of the gyration of a cross-section. As is clear from the figure for thin beam, all models, including the analytical and FEM of Timoshenko and Euler-Bernoulli theories,

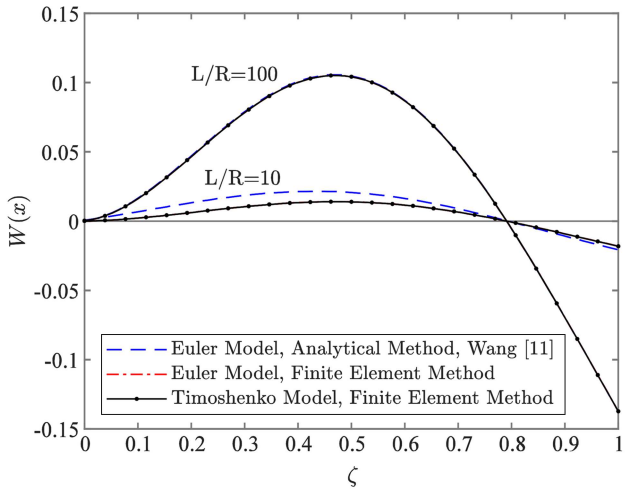

Figure 2. First mode shape of cantilever beam on intermediate elastic support.

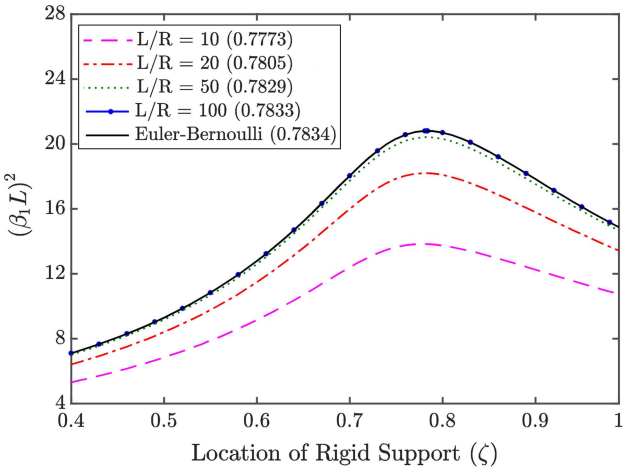

Figure 3. Based on the rigid support first natural frequency.

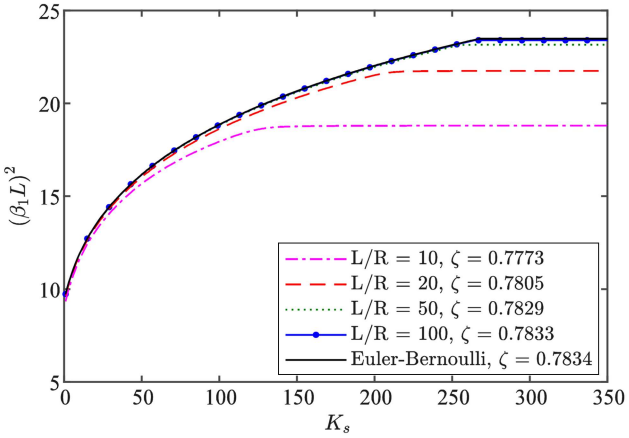

Figure 4. The first natural frequency versus support stiffness for cantilever beam.

are coincident. Nevertheless, there is a remarkable difference between Timoshenko and Euler-Bernoulli's models for thick beams. It might be surprising having a node in first mode shape.

5.1. Optimum position of elastic support

Courant's maximum-minimum theorem states that if rigid support is added at the beam ZSMS, the restricted beam's initial natural frequency equals the unrestricted beam's second natural frequency. We have considered rigid intermediate support at position b. Figure 3 depicts the first non-dimensionalized natural frequency versus the position of rigid support for a cantilever beam for various slenderness ratios.

It is known that the optimum position of a rigid support on a cantilever beam for Euler-Bernoulli beams is $\xi = 0.7834$ regardless of the L/R ratio. However, in the Timoshenko model, the optimum position is dependent on the slenderness ratio. Table 1 shows the value of a cantilever beam's first and second natural frequencies for an unconstrained beam. Optimum positions for other boundary conditions are tabulated in Table 2 for various values of slenderness ratios.

5.2. Minimum stiffness at the optimum position

As mentioned before, adding rigid intermediate support at the optimum position, listed in Table 2, for instance, C-F beam with optimum position 0.7834, the restricted beam's basic frequency equals the unrestricted beam's second natural frequency $(\beta L)^2 = 3.5030 \rightarrow 21.4862$. Akesson and Olhoff [4] have shown that the support does not need to be rigid to increase natural frequency to its maximum level. They showed that if the support stiffness is more significant than a "minimum stiffness" value, the fundamental frequency will be maximized.

As Figure 4 depicts, for the ratio $L/R = 20$ and $K_s = 0$, the natural frequency equals $(\beta L)^2 = 3.4370$. As the stiffness of the intermediate support increases, the natural frequency increases nonlinearly. For a

Table 1. Natural frequencies of Cantilever unconstrained beam.

	Timoshenko's model		Euler-Bernoulli model	
L/R	First mode	Second mode	First mode	Second mode
10	3.2326	14.5588	3.5160	20.0354
20	3.4370	19.1576		
50	3.5030	21.4862		
100	3.5128	21.8971		

Table 2. Optimum position of intermediate support (ξ).

End condition	L/R	Timoshenko model	Euler-Bernoulli model
C-F	10	0.7773	0.7834
	20	0.7805	
	50	0.7829	
	100	0.7833	
C-S	10	0.5292	0.5575
	20	0.5463	
	50	0.5553	
	100	0.5569	
C-C	10	0.5	0.5
	20	0.5	
	50	0.5	
	100	0.5	
S-S	10	0.5	0.5
	20	0.5	
	50	0.5	
	100	0.5	

critical value of stiffness called "minimum stiffness," $K_s = 140$, the value of the natural frequency equals the second natural frequency of the unconstrained beam, $(\beta L)^2 = 19.1576$. We call this point knee point. After the knee point, increasing support stiffness does not affect the natural frequency, and it remains constant regardless of any stiffness change. In addition, the minimum stiffness values vary for different L/R ratios and must be calculated for each case.

For the Euler-Bernoulli beam, the minimum stiffness for the cantilever beam was reported as 266.9 by Akesson and Olhoff [4] and 266.87 by Wang [5]. Using the Timoshenko model, the minimum stiffness value depends on the slenderness ratio. Table 3 shows the minimum stiffness for different boundary conditions and slenderness ratios.

When the stiffness increases after the knee point, the first natural frequency, and corresponding mode shape remain fixed, the question is, what is the effect of increasing stiffness above the knee point? Figures 5 and 6 show the variation of first and second frequencies and corresponding mode shapes of a cantilever beam for various values of intermediate support stiffness. It is astonishing that before the knee point, the second frequency remains constant, and the first frequency changes, but after the knee point, the first frequency remains fixed, and the second frequency varies.

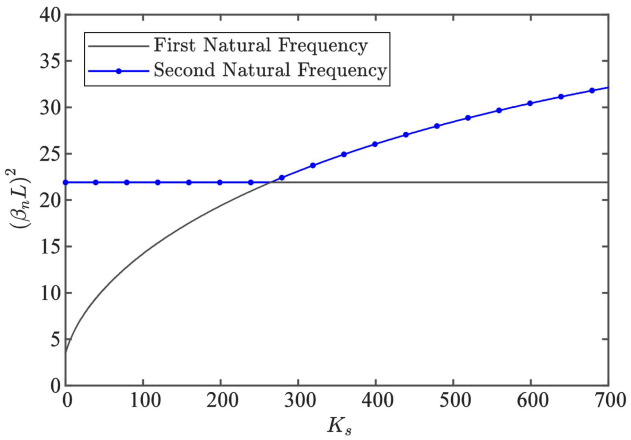

Figure 5. First and second frequencies for $L/R = 100$ and rigid support at $\xi = 0.7834$ for the cantilever beam.

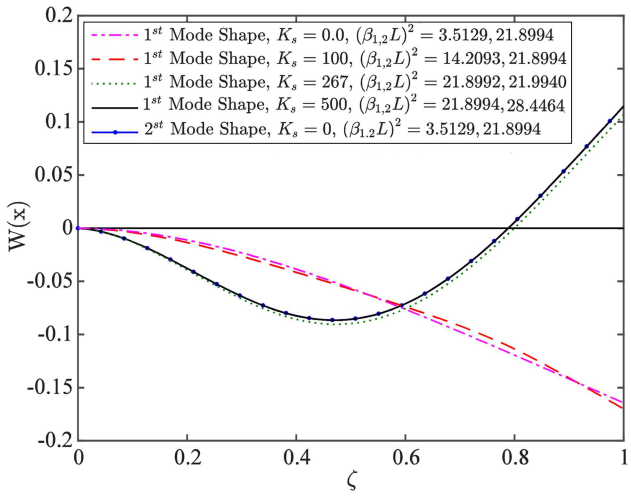

Figure 6. Comparison of first and second mode shape for stiffness value of C-F beam.

5.3. Minimum stiffness at an arbitrary position

One of the present study's most critical issues is determining the value of support stiffness to optimize the first natural frequency by placing the elastic support at an arbitrary position, which can be very useful in practical design because of practical limitations.

In many practical applications, locating support at the optimal position is impossible. In this section, we look forward to the effect of an intermediate support located at an arbitrary position.

Figure 7 shows the fundamental frequency of a cantilever beam versus support stiffness for different values of ξ and $L/R = 50$. Figure 7 depicts that for values of ξ different to 0.7834, there is no knee point, and as the stiffness increases, the natural frequency asymptotically increases to its maximum value. The maximum value corresponds to a rigid support, less than the second frequency of the unconstrained beam, as courant's theorem states.

Table 3. Minimum stiffness and raised frequency for Timoshenko model.

End condition	L/R	Minimum stiffness	Unconstrained frequency	Constrained frequency
C-F	10	138.5	3.2258	3.2258
	20	216.6	3.4351	19.0974
	50	257.08	3.5028	21.4772
	100	264.6	3.5129	21.8989
	∞	267	3.5160	22.0330
C-S	10	887.55	11.0667	27.0633
	20	1113	13.8518	39.0804
	50	1320.67	15.1344	47.5689
	100	1366.61	15.3506	49.3654
	∞	1377.65	15.4182	49.9646
C-C	10	705.57	13.8079	28.4544
	20	1271.83	18.8285	44.3008
	50	1702.60	21.6767	57.4991
	100	1800.17	22.2055	60.6146
	∞	1833.67	22.3733	61.6728
S-S	10	1017.96	8.3816	25.3097
	20	945.23	9.4095	33.5394
	50	982.4	9.7917	38.2838
	100	992.25	9.8511	39.1851
	∞	995.91	9.8696	39.4783

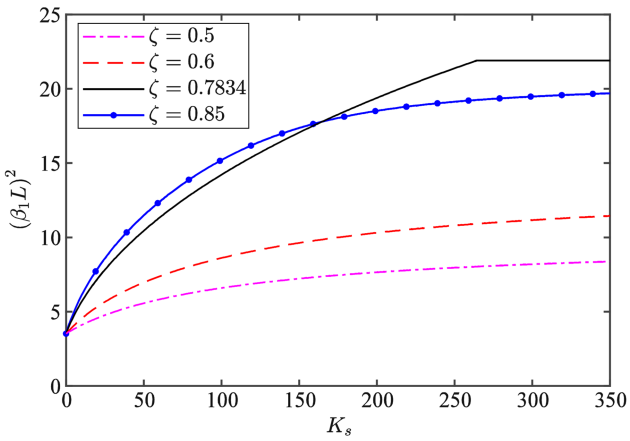

Figure 7. Frequency variation in elasticity for position support points in different locations.

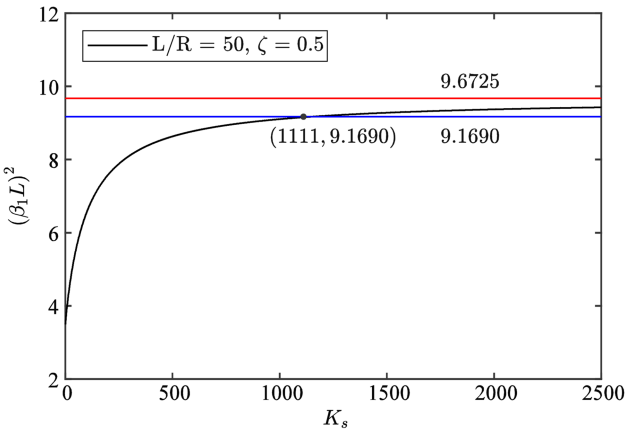

Figure 8. Introducing tolerance zone.

Here we are faced with a challenge, how can we define a minimum stiffness for non-optimally located support? We have considered a 5% tolerance zone. We define the minimum stiffness as a stiffness value that increases the first frequency to 95% of its maximum value.

Figure 8 shows the tolerance zone for a cantilever beam with $L/R = 50$ and $\xi = 0.5$. Considering 5% tolerance, the minimum stiffness and natural frequency obtain $K_s = 1111$ and $(\beta L)^2 = 9.1690$, respectively. After this point, increasing stiffness from 1111 to 2500 yields a slight increase in the frequency of about 0.3. As mentioned before, since the support position is not

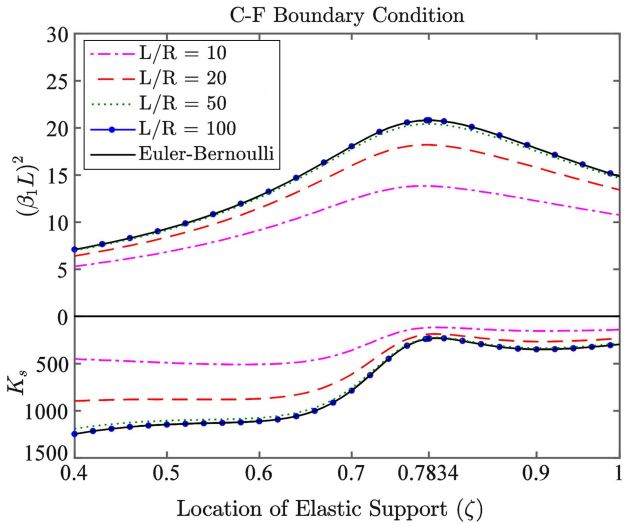

Figure 9. Design curves for C-F boundary condition.

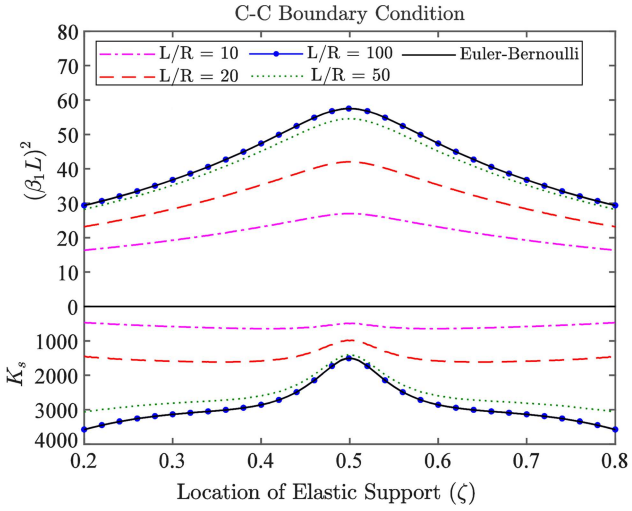

Figure 10. Design curves for C-C boundary condition.

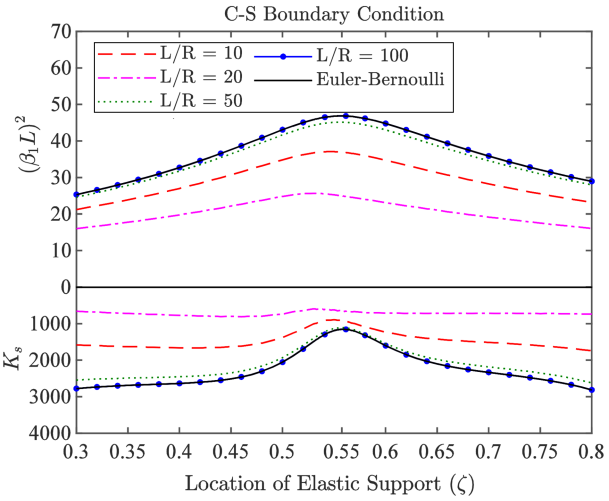

Figure 11. Design curves for C-S boundary condition.

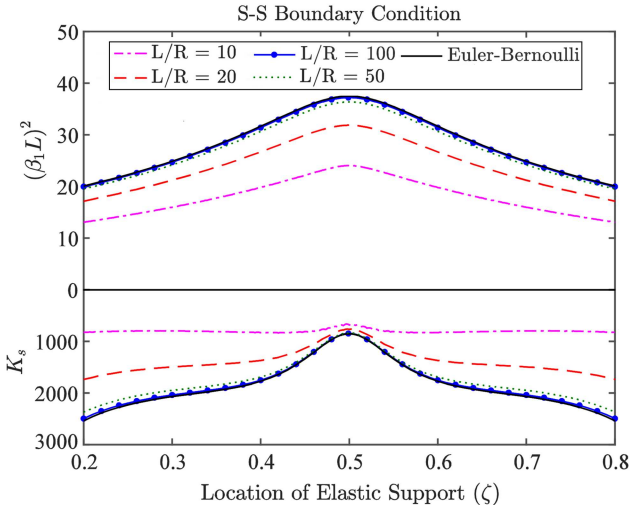

Figure 12. Design curves for S-S boundary condition.

at the optimum position, the stiffness curve has no knee point.

Figures 9–12 show the design curve based on this tolerance zone for different boundary conditions.

6. Experimental validation

Hypothetical findings are contrasted with empirical data in this section. The experiments were performed on the C-F beam, as shown in Figure 13. The dimensions of the beam specimens are 1600 and 1200 mm in length and 10 mm in diameter. The experimental setup includes an impulse hammer (Model no: 086D05 and sensitivity: 0.23 mV/N), accelerometer (Model no: IMI603 and sensitivity: 100 mV/g), and data acquisition (DAQ) board (Model no: NI4431), and signal analysis software.

The accelerometer was placed on the beam's free end to record the acceleration signals, and a hammer was used to excite the beam at 0.8L. The mass of the accelerometers is assumed to have a negligible effect. The Fast Fourier Transform (FFT) technique can be employed to process the acceleration signals once they are digitalized by the DAQ device.

Five tests are conducted. The FFTs for the case with $L = 1.2$ m are plotted in Figures 14–16. The neutral frequencies are obtained and summarized in Table 4 to further comprehend the discrepancies. A thin, long beam was employed in the tests. Due to low bending stiffness, vibration in different directions, and accelerometer measurement error at low frequencies, the natural frequency measurements have significant errors in the unsupported beams, particularly the one with a 1.6 m length. The difference between the experimental and numerical frequencies became negligible with intermediate support and increased system stiffness. It was observed that the middle support

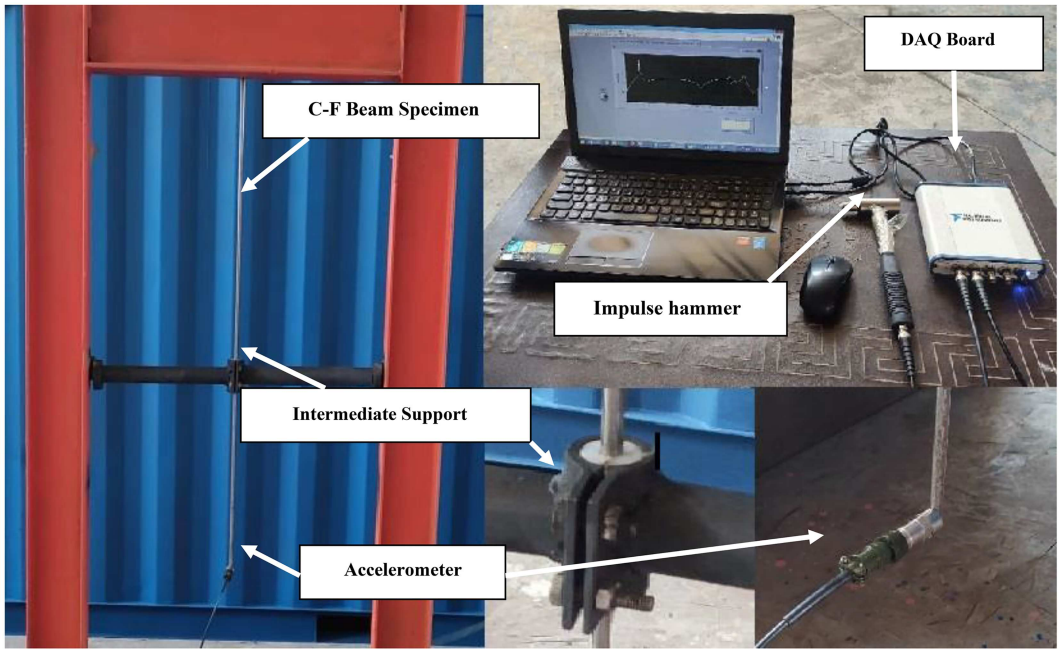

Figure 13. Experimental test setup cantilever condition.

Table 4. Comparison of experimental results and FEM.

Test no.	L (m)	ξ	x_k (m)	Natural frequency (Hz)		Difference (%)
				FEM	Experimental	
1	1.6	0	0	2.804	2.4	14.40
2		0.625	1	11.80	13.5	14.40
3	1.2	0	0	5.005	3.9	22.07
4		0.58	0.7	18.17	18.9	4.01
5		0.83	1	30.07	30.5	1.43

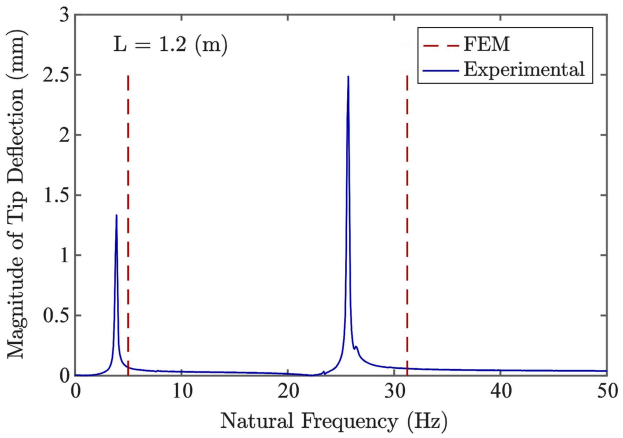

Figure 14. The frequency spectrum of the tip beam without support.

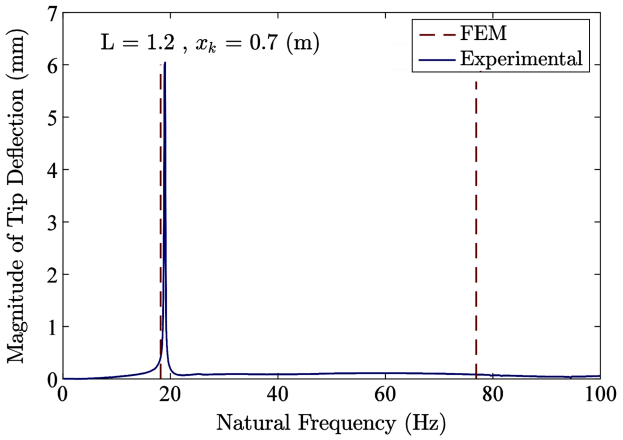

Figure 15. The frequency spectrum of the tip beam with support located at 0.7 m from the clamp end.

increased the initial natural frequency. The frequency of the beam with a length of 1.2 m was calculated to be 3.9 Hz (22% error). A place of support at 0.58L from the clamp end raised the natural frequency to 18.9 Hz. A change in the support location from 0.58L to 0.83L increased the natural frequency from 18.9 to 30.5 Hz. The negligible difference between the results could be attributed to the weight of the accelerometer.

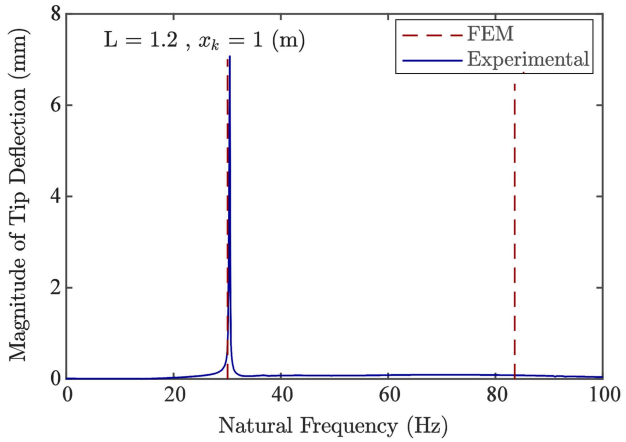

Figure 16. The frequency spectrum of the tip beam with support located at 1 m from the clamp end.

A shift in the support location toward the second-mode node of the unconstrained beam (i.e., 0.7834L) changed the frequency closer to the unrestricted beam's second natural frequency (31.24 Hz). The experimental results supported both Courant's maximum-minimum principle and numerical model. This ensures that the proposed graphs can be employed as a reference in designing beams with intermediate support under different boundary conditions.

7. Conclusions

This paper is studied the maximizing of the first natural frequency associated with the transverse vibrations of a Timoshenko's beam with rigid and elastic intermediate support. Using Courant's maximum-minimum theorem, an additional constraint was imposed on the beam. Motion equations were solved analytically and numerically using the finite element method. After validating the results through comparison to an analytical method and previous works, the impacts of the slenderness ratio and the position and stiffness of intermediate elastic supports on the fundamental frequency were investigated. It was observed that after a value of the minimum stiffness, the first natural frequency remains constant, which is completely different from the reported result of the Euler-Bernoulli beam. In many practical applications, it is not possible to add support at the optimum position. It was shown that, in this case, the frequency versus stiffness diagram has no knee point. For a 5% tolerance zone to determine the minimum stiffness and optimal frequency at different slenderness ratios and boundary conditions, the design curve was presented. These curves give us the minimum stiffness and raised natural frequency for an arbitrary position of intermediate supports.

Ultimately, empirical testing was carried out, with the findings contrasted with hypothetical estimations of the initial two natural frequencies. A great agreement in frequency values was seen when comparing the findings.

Nomenclature

A	Beam cross-section area
E	Elastic modulus
G	Shear modulus
ρ	Density
L	Beam length
I	Area moment of inertia
μ	Shear correction factor
k	Support stiffness
K_s	Dimensionless support stiffness
t	Time
x	Distance along the x axis
x_k	Location of the elastic support
ξ	Dimensionless length
$w(t)$	Lateral deflection of the beam
$\psi(t)$	Bending slope of the beam
ω	Frequency
β	Dimensionless frequency
$Prime$	Differentiation with respect to x

References

1. Courant, R. "Zur Theorie der kleinen Schwingungen", *ZAMM - Zeitschriftfür Angewandte Mathematik and Mechanik* (1992).
DOI: 10.1002/zamm.19220020406

2. Asgarikia, M. and Kakavand, F. "Minimum diameter of optimally located damping wire to maximize the fundamental frequencies of rotating blade using Timoshenko beam theory", *International Journal of Structural Stability and Dynamics*, **21**(7), 2150090 (2021).
DOI: 10.1142/S0219455421500905

3. Courant, R. and Hilbert, D. "Methods of mathematical physics", *Interscience Publishers*, New York (1953).
DOI: 10.1002/9783527617210

4. Akesson, B. and Olhoff, N. "Minimum stiffness of optimally located supports for maximum value of beam eigenfrequencies", *Journal of Sound and Vibration*, **120**(3), pp. 457–463 (1988).
DOI: 10.1016/S0022-460X(88)80218-9

5. Wang, C. "Minimum stiffness of an internal elastic support to maximize the fundamental frequency of a vibrating beam", *Journal of Sound and Vibration*, **259**(1), pp. 229–232 (2003).
DOI: 10.1006/jsvi.2002.5100

6. Olhoff, N. and Akesson, B. "Minimum stiffness of optimally located supports for maximum value of column buckling loads", *Structural Optimization*, **3**(3),

pp. 163–175 (1991).
DOI: 10.1007/BF01743073

7. Rao, C.K. "Frequency analysis of clamped-clamped uniform beams with intermediate elastic support", *Journal of Sound and Vibration*, **133**(3), pp. 502–509 (1989).
DOI: 10.1016/0022-460X(89)90615-9

8. Won, K.M. and Park, Y.S. "Optimal support positions for a structure to maximize its fundamental natural frequency", *Journal of Sound and Vibration*, **213**, pp. 801–812 (1998).
DOI: 10.1006/jsvi.1997.1493

9. Albaracin, J.M, Zannier, L., and Gross, R.O. "Some observations in the dynamics of beams with intermediate supports", *Journal of Sound and Vibration*, **271**, pp. 475–480 (2004).
DOI: 10.1016/S0022-460X(03)00631-X

10. Zhu, J. and Zhang, W. "Maximization of structural natural frequency with optimal support layout", *Struct Multidiscip Optim*, **31**, pp. 462–469 (2006).
DOI: 10.1007/s00158-005-0593-2

11. Wang, D. "Optimal design of structural support positions for minimizing maximal bending moment", *Finite Elem Anal Des*, **43**, pp. 95–102 (2006).
DOI: 20.1001.1.10275940.1391.12.3.6.5

12. Wang, D., Friswell, M.I., and Lei, Y. "Maximizing the natural frequency of a beam with an intermediate elastic support", *Journal of Sound and Vibration*, **291**(3–5), pp. 1229–1238 (2006).
DOI: 10.1016/j.jsv.2005.06.028

13. Wang, D. and Friswell, M.I. "Support position optimization with minimum stiffness for plate structures including support mass", *Journal of Sound and Vibration*, **499**, 116003 (2021).
DOI: 10.1016/j.jsv.2021.116003

14. Kong, J. "Vibration of isotropic and composite plates using computed shape function and its application to elastic support optimization", *Journal of Sound and Vibration*, **326**(3–5), pp. 671–686 (2009).
DOI: 10.1016/j.jsv.2009.05.022

15. Wang, D., Yang, Z., and Yu, Z. "Minimum stiffness location of point support for control of fundamental natural frequency of rectangular plate by Rayleigh-Ritz method", *Journal of Sound and Vibration*, **329**(14), pp. 2792–2808 (2010).
DOI: 10.1016/j.jsv.2010.01.034

16. Aydin, E. "Minimum dynamic response of cantilever beams supported by optimal elastic springs", *Structural Engineering and Mechanics*, **51**(3), pp. 377–402 (2014).
DOI: 10.12989/sem.2014.51.3.377

17. Aydin, E., Dutkiewicz, M., Oztürk, B., et al. "Optimization of elastic spring supports for cantilever beams", *Struct Multidiscip Optim*, **62**, pp. 55–81 (2020).
DOI: 10.1007/s00158-019-02469-3

18. Roncevic, G.S., Roncevic, B., Skoblar, A., et al. "Closed form solutions for frequency equation and mode shapes of elastically supported Euler-Bernoulli beams", *Journal of Sound and Vibration*, **457**, pp. 118–138 (2019).
DOI: 10.1016/j.jsv.2019.04.036

19. Abdullatif, M. and Mukherjee, R. "Effect of intermediate support on critical stability of a cantilever with non-conservative loading, some new results", *Journal of Sound and Vibration*, **485**, 115564 (2020).
DOI: 10.1016/j.jsv.2020.115564

20. Kukla, S. "Free vibrations of axially loaded beams with concentrated masses and intermediate elastic supports", *Journal of Sound and Vibration*, **172**(4), pp. 449–458 (1994).
DOI: 10.1006/jsvi.1994.1188

21. Lin, H.P. and Chang, S. "Free vibration analysis of multi-span beams with intermediate flexible constraints", *Journal of Sound and Vibration*, **281**(2), pp. 155–169 (2005).
DOI: 10.1016/j.jsv.2004.01.010

22. Lin, H.Y. "Dynamic analysis of a multi-span uniform beam carrying a number of various concentrated elements", *Journal of Sound and Vibration*, **309**(1), pp. 262–275 (2008).
DOI: 10.1016/j.jsv.2007.07.015

23. Magrab, E.B. "Natural frequencies and mode shapes of Timoshenko beams with attachments", *Journal of Vibration and Control*, **13**, pp. 905–934 (2007).
DOI:10.1177/1077546307078828

24. Han, F., Dan, D., and Deng, Z. "A dynamic stiffness-based modal analysis method for a double-beam system with elastic supports", *Mechanical System and Signal Process*, **146**, 106978 (2021).
DOI: 10.1016/j.ymssp.2020.106978

25. Lei, Y., Gao, K., Wang, X., et al. "Dynamic behaviors of single- and multi-span functionally graded porous beams with flexible boundary constraints", *Applied Mathematical Modelling*, **83**, pp. 754–76 (2020).
DOI: 10.1016/j.apm.2020.03.017

26. Kukla, S. "The Green function method in frequency analysis of a beam with intermediate elastic supports", *Journal of Sound and Vibration*, **149**, pp. 154–9 (1991).
DOI: 10.1016/0022-460X(91)90920-F

27. Roncevic, G.S., Roncevic, B., Skoblar, A., et al. "A comparative evaluation of some solution methods in free vibration analysis of elastically supported beams", *Journal of Polytech Rijeka*, **6**, pp. 285–98 (2018).
DOI: 10.31784/zvr.6.1.5

28. Luo, J., Zhu, S., and Zhai, W. "Exact closed-form solution for free vibration of Euler-Bernoulli and Timoshenko beams with intermediate elastic supports", *International Journal of Mechanical Sciences*, **213**, 106842 (2022).
DOI: 10.1016/j.ijmecsci.2021.106842

29. Han, S.M., Benaroya, H., and Wei, T. "Dynamics of transversely vibrating beams using four engineering theories", *Journal of Sound and Vibration*, **225**(5), pp. 935–988 (1999).
DOI: 10.1006/jsvi.1999.2257

30. Zohoor, H. and Kakavand, F. "Vibration of Euler-Bernoulli, and beams in large overall motion on flying support using finite element method", *Scientia Iranica*, **19**(4), pp. 1105–1116 (2012).
DOI: 10.1016/j.scient.2012.06.019

Biographies

Hossein Ebrahimi received his master's degree in mechanical engineering from Arak Islamic Azad University in 2012, at present he is PhD student of IAU, Takestan Branch, Iran in Mechanical Engineering. His research interests include mechanical vibration and optimization.

Farshad Kakavand received his PhD in Mechanical Engineering from Sharif University of technology in 2011. He is an Assistant Professor at the Department of Engineering, IAU, Takestan Branch, Iran. His research interests include mechanical vibration, nonlinear dynamics and optimization.

Hassan Seidi received his PhD in Nanotechnology from National Academy of Science of Belarus in the State Scientific-Practical Materials Research Centre in 2014. He is an Assistant Professor of Mechanical Engineering at IAU, Takestan Branch, Iran. His current research focuses on mechanical properties characterization of composite and Nano composites.